

Pseudogap and Short-Range Antiferromagnetic Correlation Controlled Fermi Surface in Underdoped Cuprates: From Fermi Arc to Electron Pocket

Takao MORINARI*

Yukawa Institute for Theoretical Physics, Kyoto University, Kyoto 606-8502, Japan

Motivated by recent quantum oscillation observations in the underdoped high-temperature superconductors, the effect of the short-range antiferromagnetic correlations on the electronic properties of the short-ranged d-density wave state is investigated. At intermediate d-density wave correlations, the cross section of the energy dispersion at the Fermi energy consists of hole pockets and an electron pocket. It is argued that the electron pocket feature is smeared out by the effect of the short-range antiferromagnetic correlation, which could be the reason why any electron pockets have never been observed in the angle resolved photoemission experiments. The Hall resistance is calculated for the system with the electron band and the hole band using a finite temperature formula assuming Dirac fermion spectrum for the latter. It is argued that the scattering effect in the hole band should be anomalously large or much suppressed by superconductivity correlations and/or vortex contributions to explain the recent quantum oscillation observations.

KEYWORDS: high- T_c , Fermi arc, antiferromagnetic correlation, quantum oscillation

1. Introduction

Recent quantum oscillation observations in the longitudinal and Hall resistivities under high-magnetic fields¹⁻⁴ uncovered the Fermi surface topology in the underdoped high-temperature superconductors. From the observed oscillation period, it is found that the Fermi surface consists of small pockets. Further detailed analysis of the sign change of the Hall coefficient, it was found that the negative Hall coefficient is not associated with vortices but with the electronic properties. Namely the small pocket should be an electron pocket.²

On the origin of the electron pocket, several theories have been proposed.⁵⁻⁸ Millis and Norman proposed a scenario based on a stripe order.⁵ It is argued that electron pockets should appear for intermediate stripe correlations. Chakravarty and Kee (CK) proposed a scenario for an electron pocket based on the d-density wave (DDW) state.⁷ For strong d-density wave order, the Fermi surface is arc like, whereas at moderate d-density wave order, an electron pocket appears around $(\pi, 0)$. CK computed the Hall coefficient based on a two band model including both effects of the electron pocket and the hole pockets using the $T = 0$ conductivity

*morinari@yukawa.kyoto-u.ac.jp

formula given by Ando.⁹

Contrary to the quantum oscillation results, any electron pocket has never been observed in angle resolved photoemission spectroscopy (ARPES). In ARPES, an arc-like truncated Fermi surface has been observed in the underdoped cuprates.¹⁰ So the natural question is: How can we understand the ARPES result and the quantum oscillation result consistently? In this paper, I propose that both experimental results can be understood in a unified way by taking into account the finite-range correlation effect for the antiferromagnetic correlation. As for the description of the pseudogap state, the DDW state is assumed. However, there is no long-range DDW wave order in the model because the antiferromagnetic correlation length, ξ_{AF} , is assumed to be finite. (In this sense, the state would be similar to the staggered flux correlation proposed by Wen and Lee.^{11,12})

The finite antiferromagnetic correlation length effect on the DDW state is modeled by introducing a Lorentzian distribution for the wave vectors describing the antiferromagnetic correlation as in Ref.6. In Ref.6, the conventional spin density wave correlation is assumed. But here the DDW correlation is assumed because the ratio of the gap with d-wave symmetry to the characteristic temperature for the appearance of the correlation¹³ is consistent with the scaling relation between the pseudogap and the pseudogap temperature observed in scanning tunneling spectroscopy.¹⁴

The condition for the appearance of the electron pocket is examined and we discuss the effect of finite ξ_{AF} . The electron pocket appears for moderate DDW correlations.⁷ We show that the electron pocket disappears for short ξ_{AF} . As for the quantum oscillations, we calculate the longitudinal resistivity and the Hall coefficient. Firstly, we study each band contribution separately using the finite temperature formula. Then, we calculate total resistivity and the Hall coefficient based on the two band model according to CK.⁷ We assume the conventional Landau levels for the description of the electron pocket while we assume the Landau level wave functions for the Dirac fermions for the hole pockets.

The organization of the paper is as follows. In Sec.2, we introduce the model and discuss the topology of the Fermi surface. The condition is examined for the appearance of the electron pocket. We show that the electron pocket feature is smeared out because of the short-range correlation effect. In Sec.3, the longitudinal conductivities are computed for the electron pocket and for the hole pocket. The lifetime broadening effect is discussed. The total longitudinal resistivity is calculated based on the two band model. Section 4 is devoted to Summary and Discussion.

2. Fermi Arc and Electron Pocket

Before describing the model to analyze the effect of short-range antiferromagnetic fluctuations, we describe the mean field Hamiltonian for the DDW state,¹⁵ or orbital antiferromag-

netic state.¹⁶ The Hamiltonian for the mean field state is

$$H = \sum_{\mathbf{k} \in RBZ} \begin{pmatrix} c_{\mathbf{k}\sigma}^\dagger & c_{\mathbf{k}+\mathbf{Q}\sigma}^\dagger \end{pmatrix} \times \begin{pmatrix} \varepsilon_{\mathbf{k}} - \mu & i\Delta_{\mathbf{k}} \\ -i\Delta_{\mathbf{k}} & \varepsilon_{\mathbf{k}+\mathbf{Q}} - \mu \end{pmatrix} \begin{pmatrix} c_{\mathbf{k}\sigma} \\ c_{\mathbf{k}+\mathbf{Q}\sigma} \end{pmatrix}, \quad (1)$$

where $\mathbf{Q} = (\pi, \pi)$ and

$$\begin{aligned} \varepsilon_{\mathbf{k}} &= -2t_0 (\cos k_x + \cos k_y) - 4t_1 \cos k_x \cos k_y \\ &\quad - 2t_2 (\cos 2k_x + \cos 2k_y). \end{aligned} \quad (2)$$

The lattice constant, a , is set to be unity except in making comparisons with other length scales. The summation with respect to \mathbf{k} is taken over the reduced magnetic Brillouin zone defined by $|k_x - k_y| < \pi$ and $|k_x + k_y| < \pi$. The DDW correlations are described by

$$\Delta_{\mathbf{k}} = \frac{\Delta_0}{2} (\cos k_x - \cos k_y). \quad (3)$$

The complete analysis of the effect of finite-range fluctuations requires the self-energy calculation for the Green's function with the number of components being proportional to the system size. This is a formidable task. So we introduce several approximations. First of all, we take the fluctuations are quasi-static. Since there is no antiferromagnetic long-range order, the fluctuations should be dynamical. The time scale is given by the inverse of the spin wave excitation gap. However, if the doping concentration is low then one can expect that the spin wave excitation gap is small. In that case, as pointed out in Ref.6 the time scale of the fluctuations can be long compared to the ARPES experiment time scale and the time scale of the cyclotron motion in the strong magnetic field, and such a long time scale behavior of antiferromagnetic domains is observed by neutron scattering experiments in an underdoped high-temperature superconductor.¹⁷ Secondly in order to reduce the number of components of the Green's function, we focus on a pair correlation of electrons with the wave numbers \mathbf{k} and $\mathbf{k} + \mathbf{q}$. It is necessary to include at least a pair of these electrons to incorporate the effect of coherence factors. From the self-energy calculation in the lowest order with respect to the fluctuations, we find the energy dispersion as

$$E_{\mathbf{k}}^{(\pm)} = \frac{\varepsilon_{\mathbf{k}} + \varepsilon_{\mathbf{k}+\mathbf{q}}}{2} - \mu \pm \sqrt{\left(\frac{\varepsilon_{\mathbf{k}} - \varepsilon_{\mathbf{k}+\mathbf{q}}}{2}\right)^2 + \Delta_{\mathbf{k}}^2}, \quad (4)$$

where \mathbf{q} dependence is implicit in $E_{\mathbf{k}}^{(\pm)}$. The coupling constant is included through the change of the order parameter amplitude, Δ_0 . Anisotropy arising from the fluctuations is approximately calculated by taking an average over \mathbf{q} whose distribution is given by the Lorentzian distribution with ξ_{AF}^{-1} being broadening factor of the distribution,

$$\rho(\mathbf{q}) = \frac{\xi_{AF}^{-1}/\pi}{(\mathbf{q} - \mathbf{Q})^2 + \xi_{AF}^{-2}}. \quad (5)$$

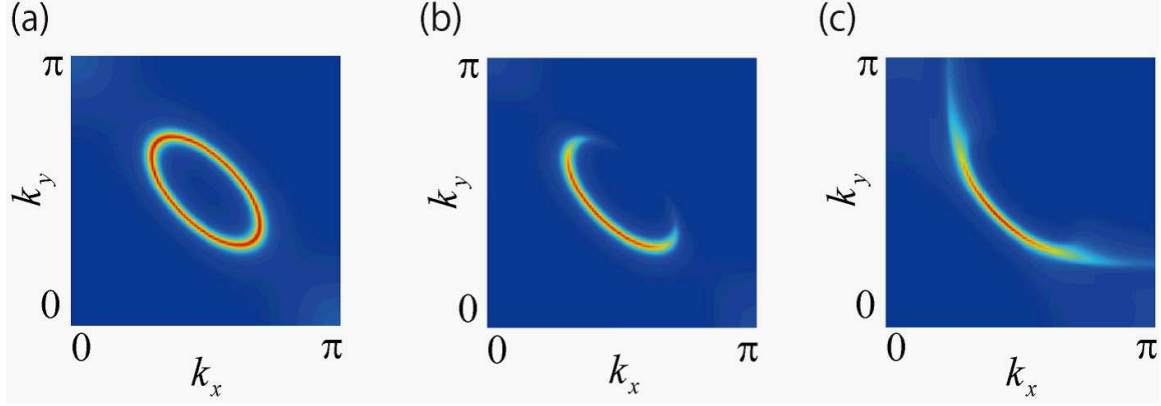


Fig. 1. (Color online) Spectral intensity at the Fermi energy calculated from eq.(6). The parameters are $t_1/t_0 = -0.25$, $t_2/t_0 = 0.10$, and $\Delta_0/t_0 = 1$. (a)Spectral intensity without the coherence factors. (b)Spectral intensity with the coherence factors. (a) and (b) are for the mean field state, $\mathbf{q} = \mathbf{Q}$. (c)Spectral intensity at $\xi_{AF}/a = 5$ with a the lattice constant.

In numerical computations for finite size systems, the normalization factor is rescaled so that $\int d^2\mathbf{q}\rho(\mathbf{q}) = 1$.

The spectral function is given by

$$-\frac{1}{\pi}\text{Im}G_{\mathbf{k}\sigma}^R(\omega) = \frac{E_{\mathbf{k}} + \varepsilon_{\mathbf{k}}^{(-)}}{2E_{\mathbf{k}}}\delta(\omega - E_{\mathbf{k}}^{(+)}) + \frac{E_{\mathbf{k}} - \varepsilon_{\mathbf{k}}^{(-)}}{2E_{\mathbf{k}}}\delta(\omega - E_{\mathbf{k}}^{(-)}), \quad (6)$$

with $\varepsilon_{\mathbf{k}}^{(\pm)} = (\varepsilon_{\mathbf{k}} \pm \varepsilon_{\mathbf{k}+\mathbf{q}})/2$, and $E_{\mathbf{k}} = \sqrt{\varepsilon_{\mathbf{k}}^{(-)2} + \Delta_{\mathbf{k}}^2}$. The factors before the delta-functions are the coherence factors associated with the DDW correlation. Hereafter the delta-functions in the right hand side of eq. (6) are replaced by a Lorentzian function, $(\Gamma/\pi)/[(\omega - E_{\mathbf{k}}^{(\pm)})^2 + \Gamma^2]$ in numerical computations, and set $\Gamma/t_0 = 0.1$. If we neglect the coherence factors, we obtain the so-called hole pockets at $\mathbf{q} = \mathbf{Q}$ as shown in Fig.1(a) for $\Delta_0/t_0 = 1$. As pointed out by Chakravarty *et al.*,¹⁸ the weight outside the reduced Brillouin zone is suppressed by including the coherence factors as shown in Fig.1(b). However, there are some deviations from the ARPES results around the end points of the arc as pointed out by Norman *et al.*¹⁹ This discrepancy is removed by decreasing ξ_{AF} as shown in Fig.1(c).

For $\Delta_0/t_0 \simeq 1$, we only see Fermi arcs. However, by decreasing Δ_0/t_0 electron pocket appears. In Fig.2, the cross section of the energy dispersion at the Fermi energy is shown for different values of Δ_0/t_0 . For small values of Δ_0/t_0 , the electron pocket is clearly seen around $(\pi, 0)$. The size of the electron pocket decreases with increasing Δ_0/t_0 . The condition for the appearance of the electron pocket is $E_{\mathbf{k}=(\pi,0)}^{(+)} = 4t_1 - 4t_2 - \mu + \Delta_0 < 0$. For $x = 0.10$ with $t_1/t_0 = -0.25$ and $t_2/t_0 = 0.10$, this condition is satisfied at $\Delta_0/t_0 = 0.7$ but not satisfied at $\Delta_0/t_0 = 0.8$.

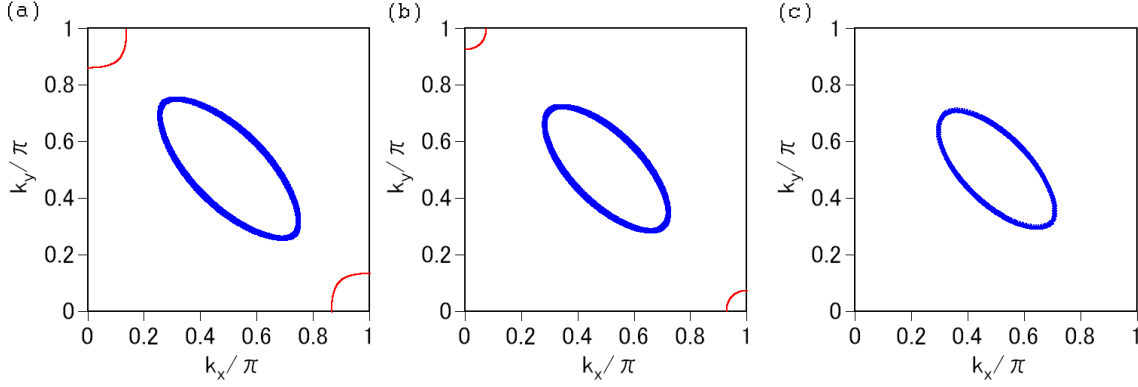


Fig. 2. (Color online) The cross section of the energy dispersion at the Fermi energy in a quadrant of the Brillouin zone: (a) $\Delta_0/t_0 = 0.5$, (b) $\Delta_0/t_0 = 0.7$, and (c) $\Delta_0/t_0 = 0.8$. The hopping parameters are the same as those in Fig.1. The thin solid lines around $(\pi, 0)$ and $(0, \pi)$ is associated with $E_{\mathbf{k}}^{(+)} = 0$, whereas the thick solid line around $(\pi/2, \pi/2)$ is associated with $E_{\mathbf{k}}^{(-)} = 0$.

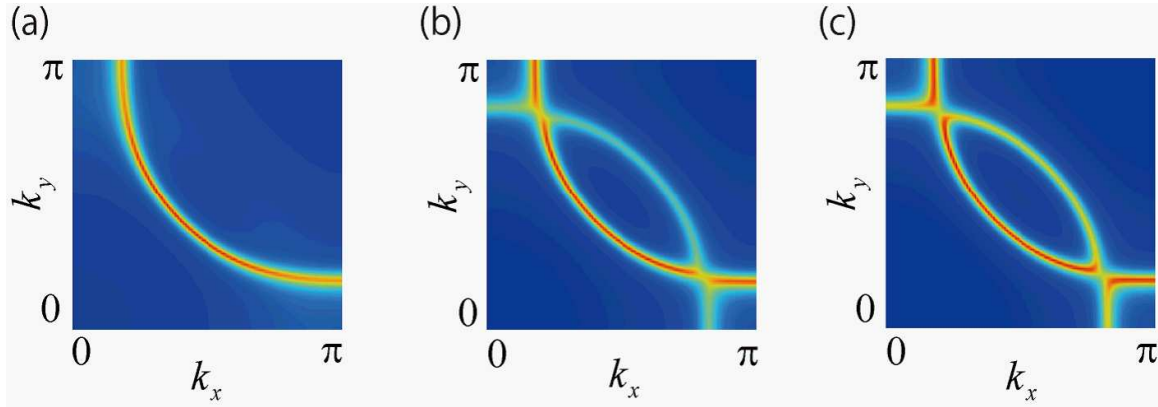


Fig. 3. (Color online) Spectral intensity at (a) $\xi_{AF}/a = 2$, (b) $\xi_{AF}/a = 50$, and (c) $\xi_{AF}/a = 100$. $\Delta_0/t_0 = 0.20$ for all panels. Coherence factors are turned off to make clear the separation between the electron pocket and the hole pocket.

Although the existence of the electron pocket is consistent with the recent quantum oscillation observations, such a pocket has never been observed in ARPES measurements so far.²⁰ In order to understand this point, the spectral weights for several values of ξ_{AF} are shown in Fig.3. For short ξ_{AF} , the electron band merges into Fermi arcs and make a full Fermi surface. By increasing ξ_{AF} , there appears a clear separation between the Fermi arc and the electron band. Thus, the electron pocket disappears for short ξ_{AF} . The qualitative difference of the spectral intensity at the Fermi energy on Δ_0/t_0 and ξ_{AF}/a plane is summarized in Fig.4.

3. Shubnikov-de Haas Oscillation

Now we discuss the Shubnikov-de Haas oscillation associated with the electron pocket. In the experimental observation by Doiron-Leyraud *et al.*,¹ the quantum oscillation is observed

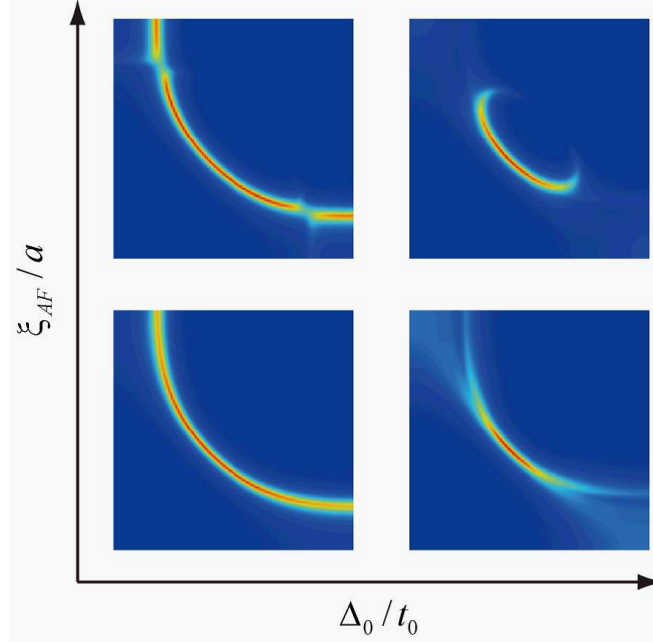


Fig. 4. (Color online) Summary of Δ_0/t_0 and ξ_{AF}/a dependence of the spectral weight. For small ξ_{AF}/a and Δ_0/t_0 , the full Fermi surface is seen. For small ξ_{AF}/a but large Δ_0/t_0 , the Fermi surface is truncated, and becomes an arc. For large ξ_{AF}/a and small Δ_0/t_0 , the energy band is separated into two bands: One is the hole band and the other is the electron band. The energy bands themselves form closed paths at the Fermi energy. For large ξ_{AF}/a and large Δ_0/t_0 , there is no electron band, and there are some rounded feature around the end points of the arc.

both in the longitudinal resistivity and the Hall resistivity. First we consider the former and next we discuss the latter. In order to include the finite temperature effect, we use the following formula for the longitudinal conductivity,

$$\sigma_{xx} = \frac{2\pi e^2}{h} \int dE \left(-\frac{\partial f}{\partial E} \right) \sum_{n=0}^{\infty} (n+1) \frac{\hbar\omega_c\Gamma/\pi}{(E - E_n)^2 + \Gamma^2} \times \frac{\hbar\omega_c\Gamma/\pi}{(E - E_{n+1})^2 + \Gamma^2}. \quad (7)$$

Here spin degeneracy is included and $E_n = (n + 1/2)\hbar\omega_c$ are the Landau level energies. The derivation is given in Appendix. In the numerical computations, the summation over Landau levels is taken up to $n = 200$. In this formula, the chemical potential, μ , the constant inelastic scattering parameter Γ , and the effective mass m^* are the parameters.

In the experiment, the period of the magnetic oscillation is estimated to be $\Delta B = 530\text{T}$.¹ This implies that the Fermi surface area is $A_k = 0.076\pi^2$. This value is obtained for the electron pocket at $\Delta_0/t_0 = 0.442$ for the parameters of $t_1/t_0 = -0.25$ and $t_2/t_0 = 0.10$. On the other hand, the hole pocket takes $A_{hp} = 0.138\pi^2$. The Luttinger sum rule is satisfied because there are two hole pockets and one electron pocket in the reduced Brillouin zone as discussed by CK.⁷ In this parameter set, the chemical potential is $\mu/t_0 = -0.750$. For the

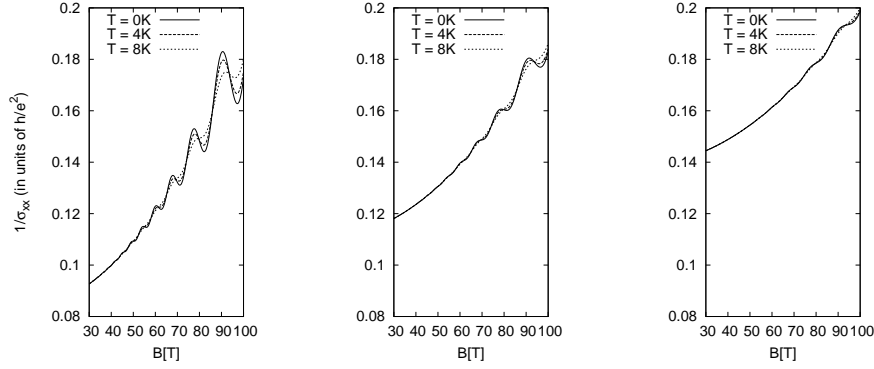


Fig. 5. The inverse of σ_{xx} for the electron pocket versus magnetic field for different temperatures. The left panel is for $\Gamma = 30\text{K}$, the middle panel is for $\Gamma = 40\text{K}$, and the right panel is for $\Gamma = 50\text{K}$.

electron pocket, the bottom of the band energy is at $E_{(\pi,0)}^{(+)} = -1.4t_0 - \mu + \Delta_0 \simeq -0.21t_0$. This should be equal to $\hbar\omega_c \times \Delta B$. Assuming $m^*/m = 2$ and $\Delta B = 530\text{T}$, we find $E_{(\pi,0)}^{(+)} = -360\text{K}$ and $t_0 \simeq 1700\text{K}$.

In Fig. 5 the inverse of σ_{xx} for the electron pocket is shown. In the experiments, the oscillation is observed from $B \simeq 50\text{T}$. To reproduce this behavior Γ should satisfy $\Gamma \leq 30\text{K}$ as seen in Fig.5. The characteristic magnetic field above which the oscillation is observed is scaled by Γ . This behavior is understood from the fact that to observe the oscillating behavior the separation of the Landau levels is larger than the Landau level broadening.

Next we consider the contribution from the hole pocket. We describe the holes as Dirac particles because the energy dispersion around $(\pi/2, \pi/2)$ is well described by a relativistic form. The necessary parameters for the anisotropic dispersion form discussed in Ref.16 are evaluated from the shape of the hole pocket. Rotating by $-\pi/4$ about the origin in the k_x - k_y plane, the hole pocket is described by $\frac{(k_X - \pi/\sqrt{2})^2}{a^2} + \frac{k_Y^2}{b^2} = 1$. Here we take the rotated axis as k_X and k_Y . The hole pocket is fitted by taking $a = 0.133\pi$ and $b = 0.34\pi$. The approximate energy dispersion is $E_{\mathbf{k}}^D = \sqrt{c_X^2 (k_X - \pi/\sqrt{2})^2 + c_Y^2 k_Y^2}$. The parameter c_X is associated with the DDW state through $c_X = \sqrt{2}\Delta_0$.¹⁶ Setting $\Delta_0 = 750\text{K}$, we find $c_X \simeq 1100\text{K}$ and $c_Y = (0.34\pi/0.133\pi)c_X \simeq 2700\text{K}$. The Landau levels are¹⁶

$$E_n = \text{sgn}(n) \sqrt{\frac{2eB}{c\hbar} a^2 c_X c_Y |n|}, \quad (8)$$

with $n = 0, \pm 1, \pm 2, \dots$, where the lattice constant a is recovered. Substituting above estimated values, we obtain

$$E_n \simeq 35\sqrt{nB}. \quad (9)$$

Here B is measured in units of tesla and E_n is measured in units of kelvin. From the value of $A_{hp} = 0.138\pi^2$, the oscillation period associated with the hole pocket is 970T from the Onsager relation as discussed by CK.⁷ In order to fit with this oscillation period, the dispersion energy is shifted so that the chemical potential for the holes is at $\mu_h \simeq 1100\text{K}$. The formula

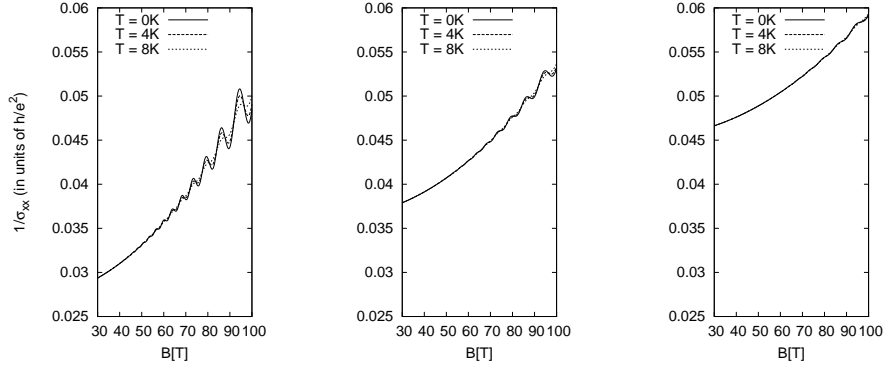


Fig. 6. The inverse of σ_{xx} for the hole pocket versus magnetic field for different temperatures. The left panel is for $\Gamma = 30\text{K}$, the middle panel is for $\Gamma = 40\text{K}$, and the right panel is for $\Gamma = 50\text{K}$.

for the longitudinal conductivity under the magnetic field is obtained by computing the matrix elements of the Dirac fermion current operators and taking eq.(9) for E_n . (For explicit derivation and discussions about impurity scattering effect, see, Ref.21.) For degeneracy, we include valley degeneracy as well as spin degeneracy. In the reduced Brillouin zone, the hole pockets around $(\pi/2, \pi/2)$ and $(-\pi/2, -\pi/2)$ are equivalent. The same is true to those around $(\pi/2, -\pi/2)$ and $(-\pi/2, \pi/2)$. However, the hole pockets around $(\pi/2, \pi/2)$ and $(\pi/2, -\pi/2)$ should be distinguished. Therefore, to incorporate this degeneracy the formula is multiplied by the factor of two. The inverse of σ_{xx} for the holes is shown in Fig.6 for different Γ 's. The behavior is qualitatively similar to that for the electron pocket.

Now we move on to the total Hall coefficient. From Fig.5, we see that Γ for the electron band, Γ_e , should be less than 30K to observe the quantum oscillation from $B \simeq 50\text{T}$. Therefore, we fix $\Gamma_e = 30\text{K}$ in the following analysis. The remaining parameter is Γ for the hole band, Γ_h . We compute the total Hall coefficient based on the two band formula,

$$R_H = \frac{R_H^e (\sigma_{xx}^e)^2 + R_H^h (\sigma_{xx}^h)^2 + (\sigma_{xx}^e)^2 (\sigma_{xx}^h)^2 R_H^e R_H^h (R_H^e + R_H^h) B^2}{(\sigma_{xx}^e + \sigma_{xx}^h)^2 + (\sigma_{xx}^e)^2 (\sigma_{xx}^h)^2 B^2 (R_H^e + R_H^h)^2}, \quad (10)$$

assuming σ_{xx} 's for each band and $R_H^e = -1/n_e|e|c$ and $R_H^h = 1/n_h|e|c$ for the Hall coefficients of the electron band and the hole band, respectively following CK. Here the particle densities are $n_e = A_{ep}/(2\pi^2)$ and $n_h = A_{hp}/\pi^2$. The difference from CK is that we use the finite temperature formula for the computation of the conductivities and take into account the Dirac fermion properties of the hole band. From the computation of R_H for various Γ_h we find that the behavior of R_H changes largely depending on Γ_h . The total Hall coefficient is shown in Fig.7 for $\Gamma_h = 200\text{K}$, $\Gamma_h = 400\text{K}$, and $\Gamma_h = 1000\text{K}$. For $\Gamma_h = 200\text{K}$, $|R_H|$ decreases as increasing B . While for $\Gamma_h = 400\text{K}$, $|R_H|$ shows an oscillating behavior. But the amplitude is very small because of the cancellation between the electron pocket contribution and the hole pocket contribution. To reproduce the experimental results, Γ_h should be $\Gamma_h \geq 1000\text{K}$. Therefore, there should be strong scattering in the hole band. Although the origin of such

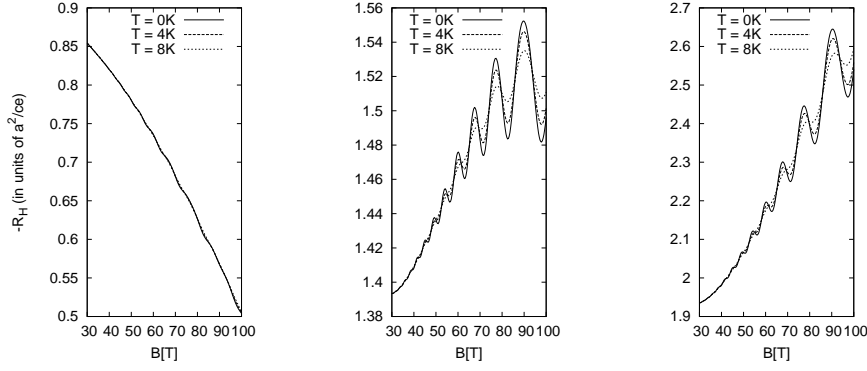


Fig. 7. The total Hall coefficient versus magnetic field for different temperatures. The scattering parameter Γ_h 's are $\Gamma_h = 200\text{K}$ for the left panel, $\Gamma_h = 400\text{K}$ for the middle panel, and $\Gamma_h = 1000\text{K}$ for the right panel.

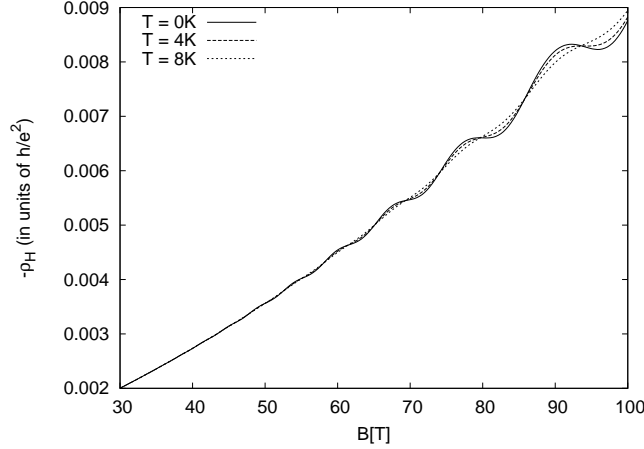


Fig. 8. The total Hall resistance versus magnetic field for different temperatures. The scattering parameters are $\Gamma_e = 30\text{K}$ and $\Gamma_h = 1000\text{K}$.

a scattering is not clear, if this is the case the oscillation associated with the hole pocket is not observable. Because we need unrealistically huge magnetic field to observe the quantum oscillations associated with the hole pocket for such large values of Γ_h . In Figs.8 and 9, the total Hall resistance and the longitudinal resistivity at $\Gamma_h = 1000\text{K}$ are shown, respectively.

Now we discuss the finite ξ_{AF} effect on the quantum oscillation. The distribution of the electron pocket and the hole pocket areas in the wave vector space is computed by taking the average over the Lorentz distribution function with respect to \mathbf{q} . The same analysis is carried out for the hole pocket in the case of the spin density wave state by Harrison *et al.*⁶ The result is well fitted by the Lorentz function. This Lorentz form suggests that the oscillating component amplitude decays rapidly in the low magnetic field as $\exp(-2\pi\delta B_0/B)$ with $\delta B_0 = 7 \times 10^3 \delta A_k / \pi^2$. Here δA_k is the half value of width of the Lorentz distribution. The Lorentz function fits for the electron pocket and the hole pocket distributions are shown

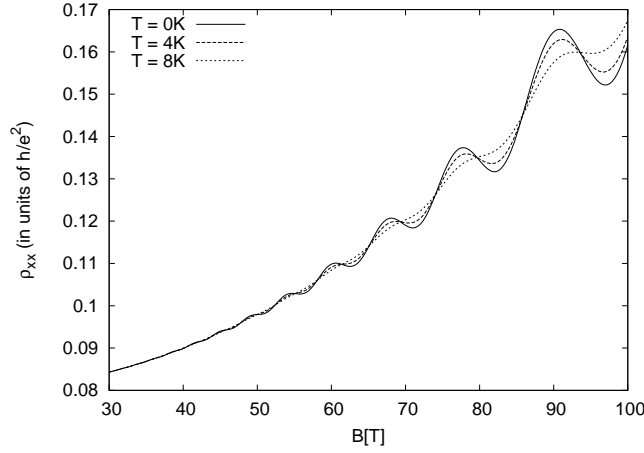


Fig. 9. The total longitudinal resistivity versus magnetic field for different temperatures. The scattering parameters are $\Gamma_e = 30\text{K}$ and $\Gamma_h = 1000\text{K}$.

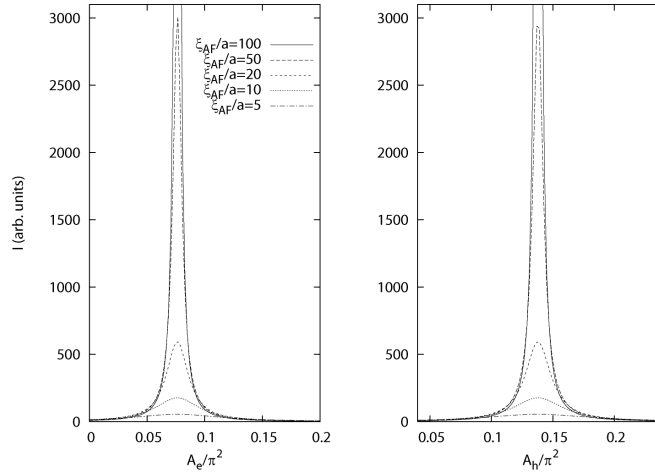


Fig. 10. Probability distributions of the electron pocket and hole pocket areas A_e and A_h in the wave vector space for $\xi_{AF}/a = 100, 50, 20, 10, 5$.

in Fig.10 for different values of ξ_{AF}/a . We see that at $B = 60\text{T}$ the oscillation amplitude is reduced to 20% at $\xi_{AF}/a = 100$ and 4% at $\xi_{AF}/a = 50$. This analysis suggests that to observe the quantum oscillation we need sufficiently long ξ_{AF} . This point is first emphasized by Harrison *et al*⁶ from the analysis of the hole pocket.

4. Summary and Discussion

In this paper, we have studied the effect of the short-range antiferromagnetic correlation on the short-ranged DDW state. For $\Delta_0/t_0 \sim 1$, the Fermi surface is arc-like and there is no electron pocket. For moderate values of Δ_0/t_0 , an electron pocket appears. The effect of the short-range antiferromagnetic correlation on the electron pocket depends on the value of ξ_{AF}/a . For $\xi_{AF}/a \sim O(1)$, the electron pocket is smeared out and is combined with the

Fermi arc so that the resulting Fermi surface is the full Fermi surface. While for $\xi_{AF}/a \gg 1$, the electron pocket feature is preserved. We apply this observation to the recent quantum oscillation result and the ARPES results. The presence of an electron pocket is suggested from the recent quantum oscillation measurements¹⁻⁴ in high magnetic fields. By contrast, any electron pocket has never been observed in ARPES. This apparent contradiction is resolved if we assume that in high magnetic fields Δ_0/t_0 decreases and ξ_{AF}/a increases.

As argued by Harrison *et al.*, long ξ_{AF} in high magnetic fields is consistent with the neutron scattering experiments and ξ_{AF} can be long at high magnetic fields because of enhancement of antiferromagnetic correlations around vortices. However, the magnetic field effect on the value of Δ_0/t_0 is not well understood. As demonstrated by Nguyen and Chakravarty²² within the mean field theory, the magnetic field effect on Δ_0 is negligible. Therefore, to reduce the value Δ_0/t_0 we need to increase t_0 . From the study of the single hole system by a self-consistent Born approximation in the slave-fermion theory of the t-J model,²³ it is believed that the band width is strongly renormalized from the bare band width to the order of J , which is consistent with the ARPES results in the undoped cuprates.²⁴ One way to suppress the renormalization effect by magnetic field is to include the induced parallel spin configuration effects. If we use the susceptibility of the Heisenberg antiferromagnet at zero temperature,²⁵ the induced hopping amplitude due to the parallel alignment component of neighboring spins is only 10K at $B = 60\text{T}$. Although we may expect that this value increases for doped compounds, the estimation requires the analysis of the spin disordering effect. Exact diagonalizations of the $t - t' - t'' - J$ model suggest that t_0 should increase by suppressing frustration effects.²⁶

In order to examine the effect of scattering and the effect of the short-range antiferromagnetic correlation on the quantum oscillations, we have calculated the longitudinal conductivities of the electron band and the hole band. The electron band is associated with the electron pocket and the hole band is associated with the hole pocket. This splitting of the band takes place due to the antiferromagnetic correlations. We describe the Landau levels of the electron band as the conventional non-relativistic Landau levels. While we describe the hole band Landau levels as the Dirac fermion Landau levels. The parameters of the Dirac fermion dispersion are determined from the shape of the hole pocket. We have computed the longitudinal conductivity for each band. To observe the quantum oscillations from $B \simeq 50\text{T}$, the scattering parameter Γ should be less than 30K. The total Hall coefficient and the longitudinal resistivity are computed by the two band formula for the electron band and the hole band. It is found that the amplitude of quantum oscillations is rapidly suppressed by decreasing ξ_{AF} . In order to observe quantum oscillations, we need sufficiently long ξ_{AF} . For $\xi_{AF}/a = 100$, the amplitude is reduced to 20% and for $\xi_{AF}/a = 50$, the amplitude is reduced to 4%.

In addition we have found that to fit the experiments we need large Γ for the hole band.

The origin of this strong scattering is not associated with the short-range antiferromagnetic correlation effect. From the calculation of the spectral weight we see that there is broadening effect associated with the short-range antiferromagnetic correlation effect. However, the broadening is stronger for the electron band than for the hole band. Another possibility for the suppression of the hole band contribution is the superconductivity correlation and the effect of vortices. If the density of states of the hole band is reduced by superconductivity, then the hole band contribution is suppressed. In addition, vortices contribute to the longitudinal resistivity. This point requires further investigations.

In a recent experiment, de Haas-van Alphen effect is observed using a magnetic torque technique and a new oscillation period is discovered.²⁷ Podolsky and Kee proposed that the ortho-II potential in $\text{YBa}_2\text{Cu}_3\text{O}_{7-\delta}$ can lead to Fermi pockets one of which is consistent with the experiment. However, in the experiment the amplitude is much smaller than that associated with the electron pocket. In addition, the effective mass estimated from the newly found oscillation is twice as large as the effective mass estimated from the oscillation associated with the electron pocket. As for the origin of the new oscillation period, more experimental and theoretical studies would be required.

Acknowledgment

I would like to thank Profs. T. Tohyama and K. Maki for helpful discussions. This work was supported by the Grant-in-Aid for the Global COE Program "The Next Generation of Physics, Spun from Universality and Emergence" from the Ministry of Education, Culture, Sports, Science and Technology (MEXT) of Japan. and Yukawa International Program for Quark-Hadron Sciences at YITP. The numerical calculations were carried out in part on Altix3700 BX2 at YITP in Kyoto University.

Appendix: Derivation of Eq.(7)

In this appendix, we derive the formula eq.(7). From the Kubo formula, the longitudinal conductivity is given by

$$\sigma_{xx}(\omega) = \frac{1}{i\omega} [K(\omega) - K(0)], \quad (\text{A}\cdot 1)$$

where

$$K(\omega) = -\frac{1}{i\hbar S} \int_0^\infty dt e^{i\omega t - \delta t} \langle [J_x(t), J_x] \rangle_0, \quad (\text{A}\cdot 2)$$

with S the area of the system and δ being an infinitesimal positive number. Here the current operator is

$$J_x = -\frac{e}{m} \sum_j p_{jx}, \quad (\text{A}\cdot 3)$$

with p_{jx} the single particle momentum operator in the x -direction. If we neglect the interaction between the electrons, the formula is rewritten in terms of the one-body quantum states.

Taking the $\omega \rightarrow 0$ limit and noting $K(0) = ne^2/m$, the dc conductivity is

$$\begin{aligned} \sigma_{xx} &= \frac{2\pi\hbar}{S} \left(\frac{e}{m}\right)^2 \int dE \left(-\frac{\partial f}{\partial E}\right) \\ &\quad \times \sum_{\alpha} \langle \alpha | \delta(E - H) p_x \delta(E - H) p_x | \alpha \rangle. \end{aligned} \quad (\text{A}\cdot 4)$$

Here H is the one-body Hamiltonian, α denotes quantum states, and spin degeneracy is included. In the absence of the impurity scattering, the delta function part is

$$\delta(E - H) = \frac{1}{2\pi i} \left(\frac{1}{E - H - i\delta} - \frac{1}{E - H + i\delta} \right). \quad (\text{A}\cdot 5)$$

We include the scattering effect by rewriting the right hand side as

$$\frac{1}{2\pi i} \left(\frac{1}{E - H - i\Gamma} - \frac{1}{E - H + i\Gamma} \right). \quad (\text{A}\cdot 6)$$

Now we include the magnetic field effect. Under strong magnetic field, the single body quantum state is quantized into Landau levels. Taking the Landau gauge $\mathbf{A} = (0, Bx, 0)$, the wave function for the n -th Landau level with X the center coordinates is given by

$$\phi_{nX}(x) = \frac{1}{\sqrt{2^n n! \pi^{1/2} \ell_B}} H_n \left(\frac{x - X}{\ell_B} \right) \exp \left(-\frac{(x - X)^2}{2\ell_B^2} \right), \quad (\text{A}\cdot 7)$$

where $H_n(x)$ are the Hermite polynomials and $\ell_B = \sqrt{c\hbar/eB}$ is the magnetic length. The quantum states $|\alpha\rangle$ in eq.(A.4) are now $|n, X\rangle$. In terms of these eigen-states, the matrix element of the momentum operator is

$$\begin{aligned} \langle n', X' | p_x | n, X \rangle &= \frac{i\hbar}{\ell_B} \delta_{X'X} \\ &\quad \times \left(\sqrt{\frac{n+1}{2}} \delta_{n', n+1} - \sqrt{\frac{n}{2}} \delta_{n', n-1} \right). \end{aligned} \quad (\text{A}\cdot 8)$$

Substituting this formula into eq.(A.4), we obtain eq. (7). If the impurity scattering effect is included in the self-consistent Born approximation, $\Gamma \propto \sqrt{B}$ as shown in Ref.9. We do not include this effect for simplicity.

References

- 1) N. Doiron-Leyraud, C. Proust, D. LeBoeuf, J. Levallois, J. B. Bonnemaïson, R. Liang, D. A. Bonn, W. N. Hardy, and L. Taillefer: *Nature* **447** (2007) 565.
- 2) D. LeBoeuf, N. Doiron-Leyraud, J. Levallois, R. Daou, J. Bonnemaïson, N. Hussey, L. Balicas, B. Ramshaw, R. Liang, D. Bonn, W. Hardy, S. Adachi, C. Proust, and L. Taillefer: *Nature* **450** (2007) 533.
- 3) E. A. Yelland, J. Singleton, C. H. Mielke, N. Harrison, F. F. Balakirev, B. Dabrowski, and J. R. Cooper: *Phys. Rev. Lett.* **100** (2008) 047003.
- 4) A. F. Bangura, J. D. Fletcher, A. Carrington, J. Levallois, M. Nardone, B. Vignolle, P. J. Heard, N. Doiron-Leyraud, D. LeBoeuf, L. Taillefer, S. Adachi, C. Proust, and N. E. Hussey: *Phys. Rev. Lett.* **100** (2008) 047004.
- 5) A. J. Millis and M. R. Norman: *Phys. Rev. B* **76** (2007) 220503(R).
- 6) N. Harrison, R. D. McDonald, and J. Singleton: *Phys. Rev. Lett.* **99** (2007) 206406.
- 7) S. Chakravarty and H.-Y. Kee: *Proc. Natl. Acad. Sci.* **105** (2008) 8835.
- 8) W.-Q. Chen, K.-Y. Yang, T. Rice, and F. Zhang: *Europhys. Lett.* **82** (2008) 17004.
- 9) T. Ando: *J. Phys. Soc. Jpn.* **37** (1974) 1233.
- 10) M. R. Norman, H. Ding, M. Randeria, J. C. Campuzano, T. Yokoya, T. Takeuchi, T. Takahashi, T. Mochiku, K. Kadowaki, P. Guptasarma, and D. G. Hinks: *Nature* **392** (1998) 157.
- 11) X.-G. Wen and P. A. Lee: *Phys. Rev. Lett.* **76** (1996) 503.
- 12) P. A. Lee, N. Nagaosa, and X. G. Wen: *Rev. Mod. Phys.* **78** (2006) 17.
- 13) H. Won, S. Haas, D. Parker, and K. Maki: *physica status solidi(b)* **242** (2005) 181.
- 14) M. Kugler, O. Fischer, C. Renner, S. Ono, and Y. Ando: *Phys. Rev. Lett.* **86** (2001) 4911.
- 15) S. Chakravarty, R. B. Laughlin, D. K. Morr, and C. Nayak: *Phys. Rev. B* **63** (2001) 094503.
- 16) A. A. Nersisyan and G. E. Vachnadze: *J. Low. Temp. Phys.* **77** (1989) 293.
- 17) S. Hayden, G. Aeppli, H. Mook, D. Rytz, M. Hundley, and Z. Fisk: *Phys. Rev. Lett.* **66** (1991) 821.
- 18) S. Chakravarty, C. Nayak, and S. Tewari: *Phys. Rev. B* **68** (2003) 100504(R).
- 19) M. R. Norman, A. Kanigel, M. Randeria, U. Chatterjee, and J. C. Campuzano: *Phys. Rev. B* **76** (2007) 174501.
- 20) A. Damascelli, Z. Hussain, and Z. X. Shen: *Rev. Mod. Phys.* **75** (2003) 473.
- 21) N. H. Shon and T. Ando: *J. Phys. Soc. Jpn.* **67** (1998) 2421.
- 22) H. K. Nguyen and S. Chakravarty: *Phys. Rev. B* **65** (2002) 180519(R).
- 23) C. L. Kane, P. A. Lee, and N. Read: *Phys. Rev. B* **39** (1989) 6880.
- 24) B. O. Wells, Z. X. Shen, A. Matsuura, D. M. King, M. A. Kastner, M. Greven, and R. J. Birgeneau: *Phys. Rev. Lett.* **74** (1995) 964.
- 25) S. Chakravarty, B. I. Halperin, and D. R. Nelson: *Phys. Rev. Lett.* **60** (1988) 1057.
- 26) Y. Shibata, T. Tohyama, and S. Maekawa: *Phys. Rev. B* **59** (1999) 1840.
- 27) S. E. Sebastian, N. Harrison, E. Palm, T. P. Murphy, C. H. Mielke, R. Liang, D. A. Bonn, W. N. Hardy, and G. G. Lonzarich: *Nature* **454** (2008) 200.